Int. J. Electrochem. Sci., 17 **(2022)** Article Number: 221166, doi: 10.20964/2022.11.61

International Journal of
ELECTROCHEMICAL
SCIENCE
www.electrochemsci.org

Effects of Boron Carbide Particle Content on Corrosion Resistance and Wear Resistance of Ni-B/B_4C Composite Coatings

Hung-Hua Sheu[1,2,*], *Qian-You Wang*[1], *Ya-Wei Lee*[3,*]

[1] Department of Chemical and Materials Engineering, Chung Cheng Institute of Technology, National Defense University, Taoyuan City, Taiwan
[2] System Engineering and Technology Program, National Chiao Tung University, Hsin-Chu, Taiwan
[3] Department of Mechanical Engineering, Lunghwa University of Science and Technology, Taoyuan City, Taiwan
[*]E-mail: shhccit@gmail.com, yaweilee@mail.lhu.edu.tw

Received: 28 July 2022 / *Accepted:* 19 September 2022 / *Published:* 20 October 2022

In this study, Ni-B/B_4C composite coatings were prepared by adding different concentrations of B_4C particles, and the effect of B_4C particle addition on the corrosion resistance and wear resistance of composite coatings was study. The results show that the microhardness value of the composite coating does not increase with the addition content of B_4C particles. The highest microhardness value of the composite coatings occurred at the addition concentration of B_4C particle is 2 g/L, and its microhardness value is 983.7 Hv. This phenomenon can be attributed to the fact that the composite coating has the highest B_4C particle coverage (15.2 Vol.%) at this B_4C concentration. The results of corrosion resistance and wear resistance test show that the composite coatings prepared with B_4C particles at a concentration of 2 g/L has the best corrosion resistance and wear resistance, and its i_{corr} value and wear rate are 8.78×10^{-7} A/cm^2 and 2.7×10^{-4} mg/N·m, respectively. Therefore, when more B_4C particles are co-deposited in the composite coatings, the corrosion resistance and wear resistance of the composite coatings can be effectively improved at the same time.

Keywords: composite coatings, B_4C particles, corrosion resistance, wear resistance

1. INTRODUCTION

Due to its good corrosion resistance, nickel-based alloy coatings are widely used in the field of surface corrosion protection in the industry. Nickel-based alloy coatings include: pure Ni coatings [1-3], Ni-P coatings [4-6], Ni-W coatings [7,8], Ni-Co coatings [9], etc. In recent years, a novel nickel-based coating has been developed, namely the Ni-B coatings. The micro-hardness value of the Ni-B coatings is about 950 Hv, which is higher than that of the traditional Ni and Ni-P coatings, and has better wear resistance. It is an alloy coating with both good corrosion resistance and good wear resistance. Usually the boron content in the Ni-B coating is not high, the average content is below 5 at.%, and the source of boron can be divided into DMAB [10-12] and TMAB [13-15]. Since the DMAB added in the plating solution is easy to decompose and volatilize, and is relatively unstable, the boron source for preparing the Ni-B alloy coating is mainly based on the relatively stable TMAB. The reason that the microhardness value of Ni-B alloy coating is higher than that of other nickel-based alloy coatings can be attributed to the co-deposition of boron atoms into the Ni matrix during the electroplating process, resulting in a solid solution strengthening effect and increasing the microhardness of the coatings [16,17]. However, in order to improve the wear resistance of the Ni-B alloy coating again, a composite coating is formed by adding hard particles to the Ni-B alloy coating. In the 1960s, in order to improve the wear resistance of the metal coating at that time, some scholars began to add hard particles into a new type of coating in which ceramic particles and metal ions were co-deposited on the cathode during the electrodeposition process, and this coating was called composite coating. At first, the electrodeposition theory of composite coatings was divided into electrophoretic co-deposition, mechanical co-deposition and adsorption co-deposition [18], but these theories could not fully explain the co-deposition of hard particles in alloy coatings. It was not until Guglielmi [19] proposed a two-stage co-deposition mechanism in 1972 and deduced a complete mathematical model that the co-deposition process was completely explained. The first stage of loose adsorption is a physical behavior. When the particles reach the cathode, they will be loosely adsorbed on the surface of the cathode and will be in equilibrium with the suspended particles, and the particles will be surrounded by surrounding metal ions and solvent molecules. The second stage is strong adsorption, because the particles are weakly adsorbed on the cathode, but when the particles are loosened from the ion group, they will be firmly adsorbed on the surface of the cathode, so that the particles are adsorbed at the cathode, and at the same time, due to the continuous growth of metal ions, they are coated. Celis et al. [20] noticed that the Guglielmi model did not take into account the ions adsorbed by the particles, which made it impossible to explain the change of the particle content of the Cu–Al_2O_3 system with the current density. They used the data to compare the cathodic polarization curves and came to a conclusion that the particles. The rate of deposition is related to the rate of return of copper ions adsorbed on the particles. Hwang et al. [21] developed a more widely used co-deposition model when they studied the Co-SiC composite co-deposition system in 1993. They concluded that the reduction reaction of adsorbed ions on the particles is an important step in the particle deposition rate, and it was noticed that in three different current densities, the reduction characteristics of adsorbed ions are different, which leads to influence on the deposition mode of particles. This result modifies the adsorption mechanism proposed by Guglielmi, and can more reasonably explain the co-deposition method of electroplating.

Since the composite coating can improve the mechanical properties of the original alloy coating and reduce the internal stress of the coating, it has been developed in recent years. Among them, the research on the nickel-based composite coating has the most development potential. The hard particles added to the nickel-based composite coating include: SiC, Al_2O_3, Si_3N_4, diamond etc. [22-25]. The added hard particles can improve the wear resistance of the coatings, so the development of the composite coating has received great attention from the industry. The main reason why the composite coating improves the wear resistance comes from the number of hard particles co-deposited into the metal coatings. The more hard particles co-deposited, the better the wear resistance of the composite coating. Therefore, how to improve the content of hard particles in metal coatings to enhance the wear resistance of the composite coatings via various operated parameters is a very important issue. These effect factors include the concentration of the hard particles added to the plating solution, the stirred speed, the surface chargeability of the hard particles, and so on.

The hardness of boron carbide is currently known to be second only to diamond in nature, it should has well application in the preparation of composite coatings. Due to B_4C particle is difficult to co-deposited into nickel-boron alloy matrix, the application of B_4C particle in preparation of composite coatings was limited, and this pain point had been overcome in our previous study [26]. In this study, Ni-B/B_4C composite coatings were prepared by adding different concentrations of B_4C particles in the plating solution. The correlation analysis results were used to understand the effect of B_4C particle concentration in the plating solution on the corrosion resistance and wear resistance of the prepared composite coatings.

2. EXPERIMENTAL

The low carbon steel was used as substrates which had a dimension of 30 × 20 × 2 mm in this work. The composition of the electro-deposited nickel boron alloy coating is the same as the composition used in our past research, including 400 g/L nickel sulfamate ($Ni(NH_2SO_3)$), 40 g/L boric acid (H_3BO_3), 10 g/L nickel chloride ($NiCl_2 \cdot 6H_2O$), 4 g/L TMAB [26,27]. The Ni-B/B_4C composite coatings were electrodeposited from different addition concentration of B_4C particles in the bath such as 1, 2, 3, 4 and 5 g/L. The B_4C powders were prepared by our research team and its average particle size is approximately at 1.8 um. The electroplating parameters including: current density is 10 A/dm^2, electroplating temperature 25°C and electroplating duration is 20 mins. Here, the sample code is Ni-B, Ni-B/B_4C-1, Ni-B/B_4C-2, Ni-B/B_4C-3, Ni-B/B_4C-4 and Ni-B/B_4C-5, respectively. The morphologies and cross-sectional images of Ni-B/B_4C composite coatings were analyzed using a scanning electron microscopy (SEM, Jeol model JSM-6500). The hardness of composite coatings prepared from different B_4C particles added into the bath were measured by a Vickers micro-hardness tester (TECH FM-100e), the mean value for the hardness is calculated after 10 tests, loading with 25 g for 15 seconds. The potentiodynamic polarization of Ni/B_4C and Ni-B/B_4C composite coating were analyzed by a standard three-electrode cell system using an Autolab-PGSTAT30 potentiostat/galvanostat controlled by a GPES (General Purpose Electrochemical system) software and stabilized at open circuit potential (OCP) before test. The potentiodynamic polarization analysis were carried out with a 3.5 wt.% NaCl solution at room temperature. The potential was ramped from −0.8 V and 0.3 V with a scanning rate of 0.5 mV s^{-1}. The adhesion strength of Ni-B/B_4C composite coating electroplating on low carbon steel substrates were analyzed a scratch tester (Micro Scratch Tester (MST^3), Aton Paar GmbH, Germany). The load was gradually applied on Ni-B/B_4C composite coating from 0 N to 20 N, the critical load position of Ni-B/B_4C composite coating can be observed from the scratch track using optical microscopy and to define critical load of the coating.

3. RESULTS AND DISCUSSION

Fig. 1 shows the surface morphologies of Ni-B/B_4C composite coatings obtained at a fixed electrodeposition current density of 10 A/dm^2 under different B_4C particle addition concentrations (1-5 g/L).

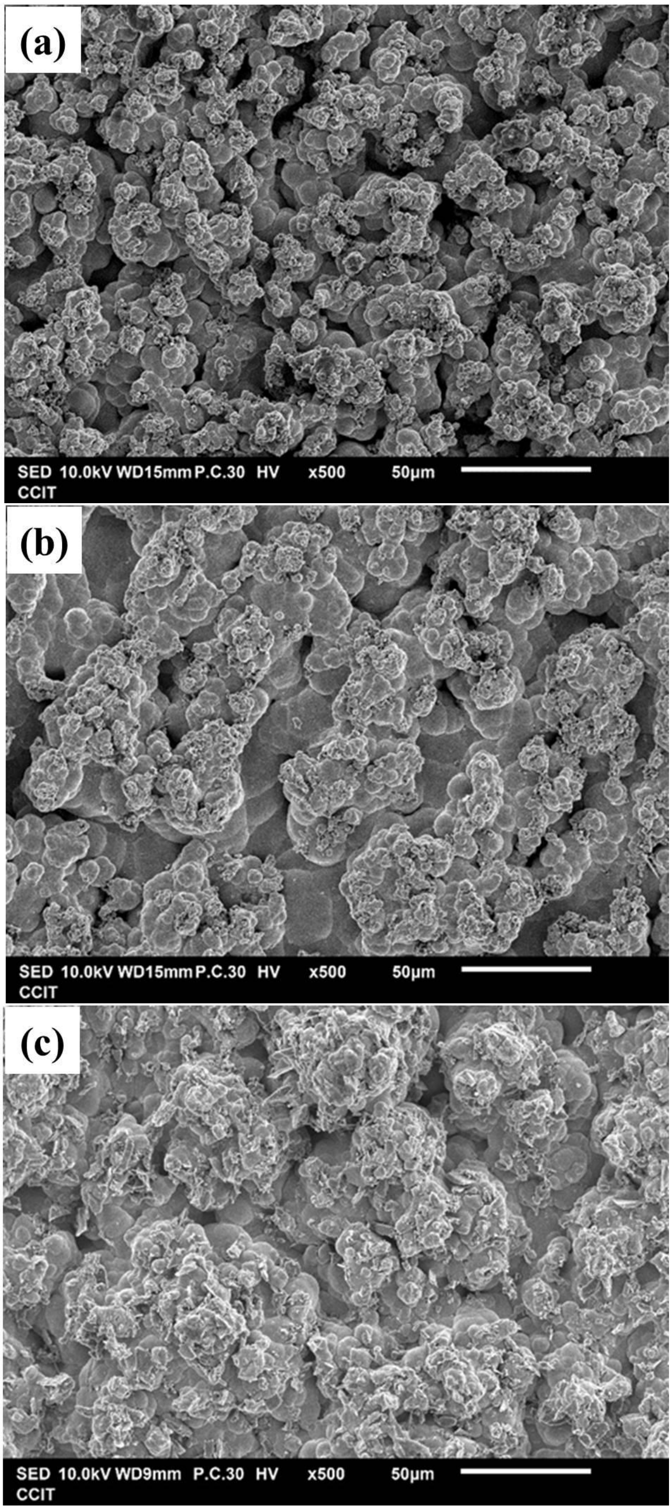

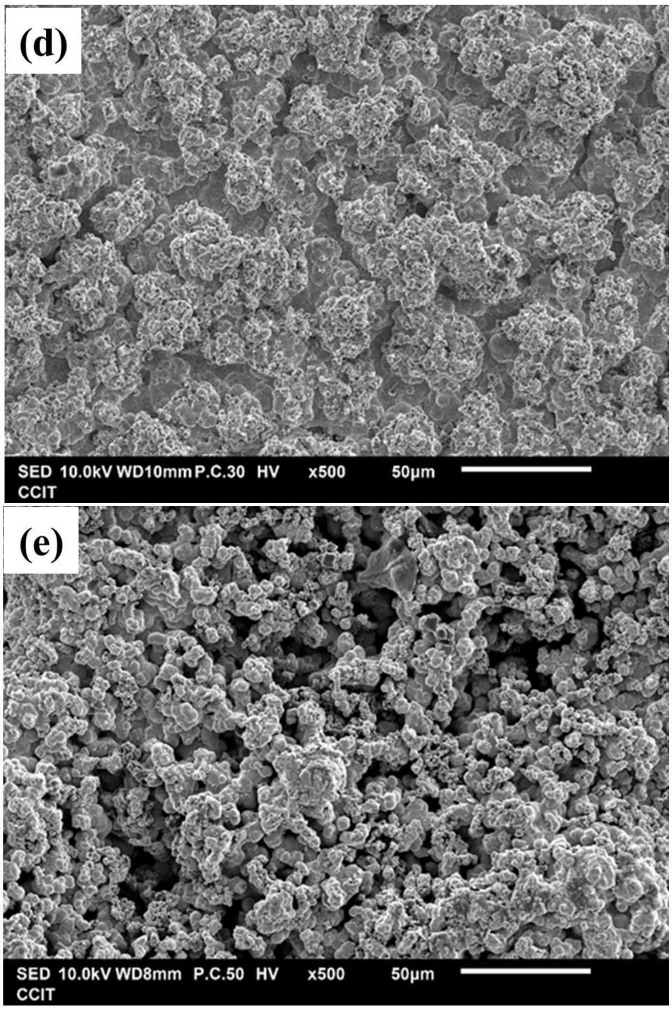

Figure 1. SEM morphologies of Ni–B/B_4C composite coatings electrodeposited from different added B_4C particles concentrations: (a) Ni-B/B_4C-1, (b) Ni-B/B_4C-2, (c) Ni-B/B_4C-3, (d) Ni-B/B_4C-4 and (e) Ni-B/B_4C-5.

It can be observed from the photos that the surface morphology of the composite coating obtained when the concentration of B_4C particles is 1 g/L and 5 g/L is loose and there are many holes and granular agglomerations (Fig. 1(a) and Fig. 1(e)). When the concentration of B_4C particles was 2 g/L, 3 g/L and 4 g/L, the surface microstructure of the obtained composite coating was denser and the pores were significantly reduced (Fig. 1(b)-(d)). However, there is still a granular structure on the surface of the coating that is agglomerated by the attraction of B_4C particles. This phenomenon has been pointed out that the surface charge of B_4C particles is affected by TMAB and caused agglomeration of B_4C particles [26].

Fig. 2 shows the cross-sectional SEM images of Ni-B/B_4C composite coatings obtained at a fixed electrodeposition current density of 10 A/dm^2 under the conditions of different B_4C particle addition concentrations (1-5 g/L). From the SEM cross-sectional photos, it can be observed that the composite coatings obtained under various B_4C particle addition conditions have B_4C particles co-deposited into the Ni-B alloy matrix. The content of B_4C particles in each composite coating was calculated by Image J image processing software, which were 7.34, 15.2, 10.7, 10.3 and 9.21 Vol. %, respectively.

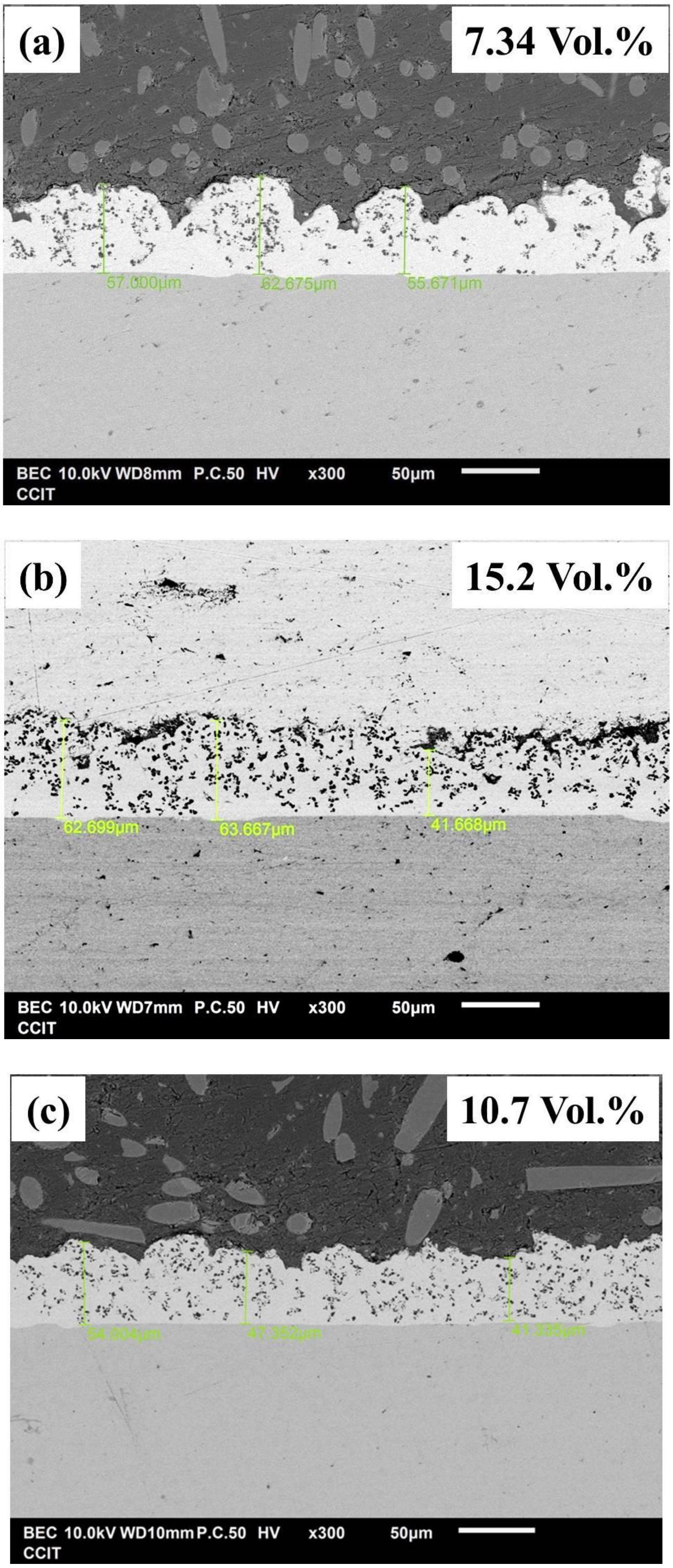
(a)
7.34 Vol.%
57.000µm
62.675µm
55.671µm
BEC 10.0kV WD8mm P.C.50 HV x300 50µm
CCIT
(b)
15.2 Vol.%
62.699µm
63.667µm
41.668µm
BEC 10.0kV WD7mm P.C.50 HV x300 50µm
CCIT
(c)
10.7 Vol.%
54.004µm
47.352µm
41.335µm
BEC 10.0kV WD10mm P.C.50 HV x300 50µm
CCIT

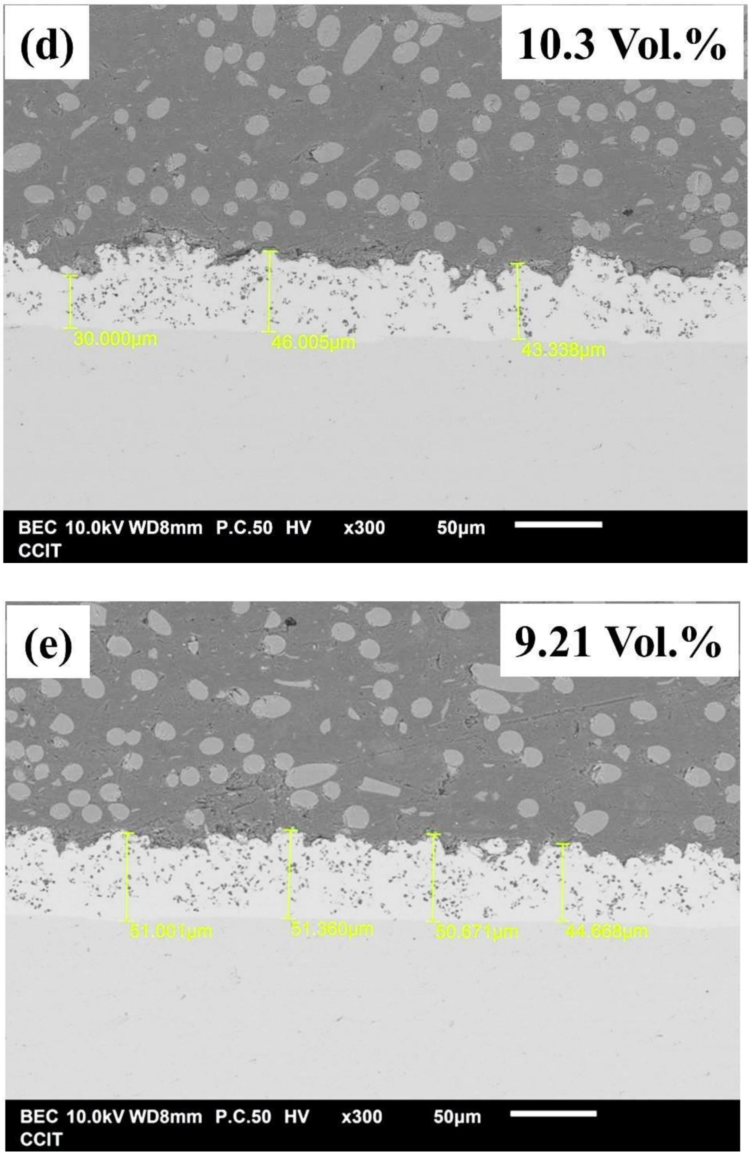

Figure 2. SEM cross-sectional images of Ni–B/B_4C composite coatings electrodeposited from different added B_4C particles concentrations: (a) Ni-B/B_4C-1, (b) Ni-B/B_4C-2, (c) Ni-B/B_4C-3, (d) Ni-B/B_4C-4 and (e) Ni-B/B_4C-5.

Table 1. Corrosion resistance of Ni-B alloy coatings and Ni-B/B_4C composite coatings electroplated from both different added concentration of B_4C particle analyzed from 3.5 wt.% NaCl solution

	B_4C particle concentration					
	0 g/L	1 g/L	2 g/L	3 g/L	4 g/L	5 g/L
E_{corr}(V vs SCE)	-0.61	–0.4	-0.4	-0.37	-0.4	-0.54
i_{corr}(A/cm^2)	9.58 x 10^{-6}	5.76 x 10^{-6}	8.78 x 10^{-7}	3.42 x 10^{-6}	4.78 x 10^{-6}	6.47 x 10^{-6}

The results show that when the concentration of B_4C particles is 1 g/L and 5 g/L, the amount of B_4C particles co-deposited into the Ni-B alloy matrix is obviously low. This indicates that the co-deposition amount of B_4C particles in the Ni-B alloy matrix does not increase with the addition of B_4C particles. In other words, under the condition of an appropriate concentration of B_4C particles added, the composite coating will have a higher amount of B_4C particles co-deposition. The experimental results show that when the concentration of B_4C particles is 2 g/L, the content of co-deposited B_4C particles in the composite coating is the highest, which can reach 15.2 Vol.%.

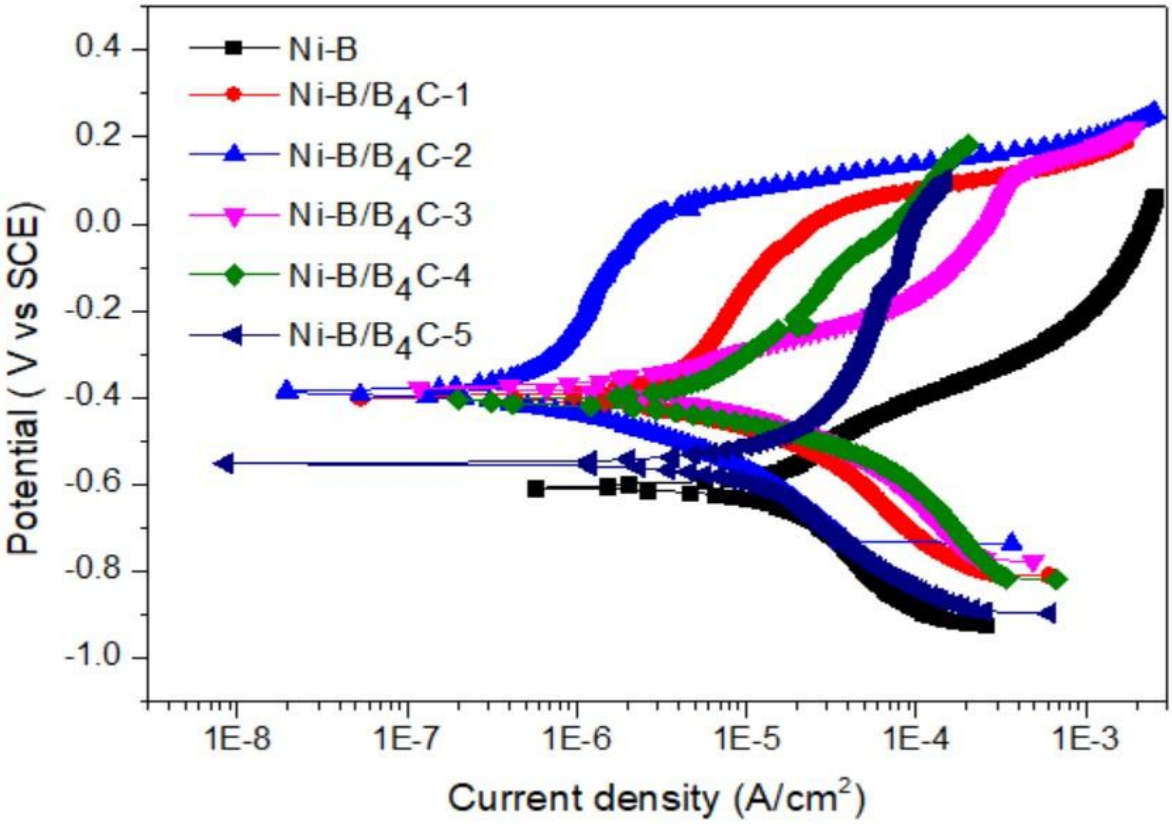

Figure 3. The polarization curves of Ni-B alloy coatings and Ni–B/B_4C composite coatings electrodeposited from different added B_4C particles concentrations, the samples including: Ni-B, Ni-B/B_4C-1, Ni-B/B_4C-2, Ni-B/B_4C-3, Ni-B/B_4C-4 and Ni-B/B_4C-5.

Fig. 3 shows the polarization curves of Ni-B/B_4C composite coatings prepared by adding different concentrations of B_4C particles. The calculated E_{corr} and i_{corr} values are shown in Table 1. The results show that the composite coating prepared with the addition of B_4C particles of 2 g/L (Ni-B/B_4C-2) has the smallest i_{corr} value of 8.78×10^{-7} A/cm^2. The i_{corr} values of Ni-B/B_4C-1 and Ni-B/B_4C-5 were higher, and their values were 5.76×10^{-6} and 6.47×10^{-6} A/cm^2, respectively. The reason for the poor corrosion resistance of the composite coating can be attributed to the loose microstructure of the composite coating prepared under the conditions of B_4C particle addition of 1 g/L and 5 g/L (as shown in Fig. 1(a) and (e)), it is easy to cause the corrosive liquid to erode down the direction of the substrate along the pores. In addition, the microstructure of the composite coating prepared when the B_4C particle addition concentration is 2 g/L is relatively dense (as shown in Fig. 1(b), which can effectively prevent corrosion factors from eroding toward the substrate and has better corrosion resistance. In the electrodeposition process, whether the prepared coating can produce effective corrosion resistance depends on whether the prepared coating can effectively reduce the formation of defects, such as pores and cracks [28,29]. Here, Ni-B alloy coatings has the worst corrosion resistance which i_{corr} value approximately equal to 9.58 x 10^{-6} A/cm^2 due to the formation of microcracks caused by internal stress of coatings. Previous literatures had indicated that adding hard particles can effectively reduce the internal stress of the coating [30-33], in this work, adding B_4C particles to the Ni-B alloy coating will also reduce the internal stress of the coating, thereby reducing the formation of microcracks, so that the corrosion resistance of the Ni-B/B_4C composite coating is better than that of the Ni-B alloy coating.

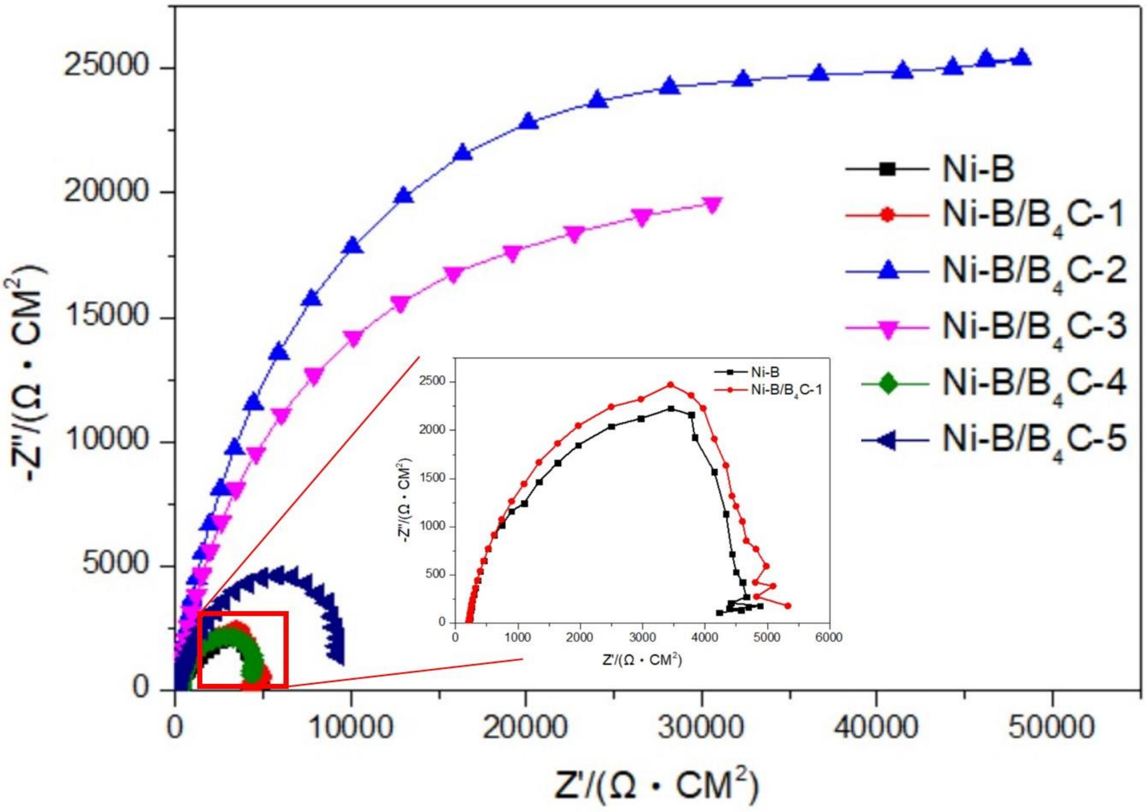

Figure 4. Nyquist plots of Ni-B alloy coatings and Ni–B/B_4C composite coatings electrodeposited from different added B_4C particles concentrations, the samples including: Ni-B, Ni-B/B_4C-1, Ni-B/B_4C-2, Ni-B/B_4C-3, Ni-B/B_4C-4 and Ni-B/B_4C-5.

Fig. 4 shows the Nyquist plots of Ni-B/B_4C composite coatings prepared with different B_4C particle concentrations. The result of Nyquist plots are consistent with the polarization curves. The figure shows that the composite coating prepared when the B_4C particle addition concentration is 2 g/L has the largest resistance value, which means that the coating has better corrosion resistance.

Generally, the microhardness value of pure nickel metal coating is about 300-500 Hv [34-36]. However, when boron atoms and nickel ions are co-deposited on the surface of the cathode, a Ni-B alloy coating with boron atoms dissolved in nickel metal is formed. Due to the effect of solid solution strengthening mechanism, the microhardness value of the Ni-B alloy coating rises significantly to about

900 Hv [16]. In this study, B_4C particles were co-deposited into the Ni-B alloy coating to form a Ni-B/B_4C composite coating. The results showed that the microhardness value of the Ni-B/B_4C composite coating was higher than that of the Ni-B alloy coating. The average microhardness of Ni-B alloy coatings is 932.6 Hv, all the average microhardness of Ni-B/B_4C composite coatings is greater than 950 Hv. This phenomenon can be attributed to the two strengthening mechanisms of solid solution strengthening and dispersion strengthening in the composite coating, which promote the composite coating to obtain a higher microhardness value [23]. The microhardness measurement results show that the Ni-B/B_4C composite coating prepared from B_4C particles with a concentration of 2 g/L has the highest microhardness value, which is approximately at 983.7 Hv (see Fig. 5).

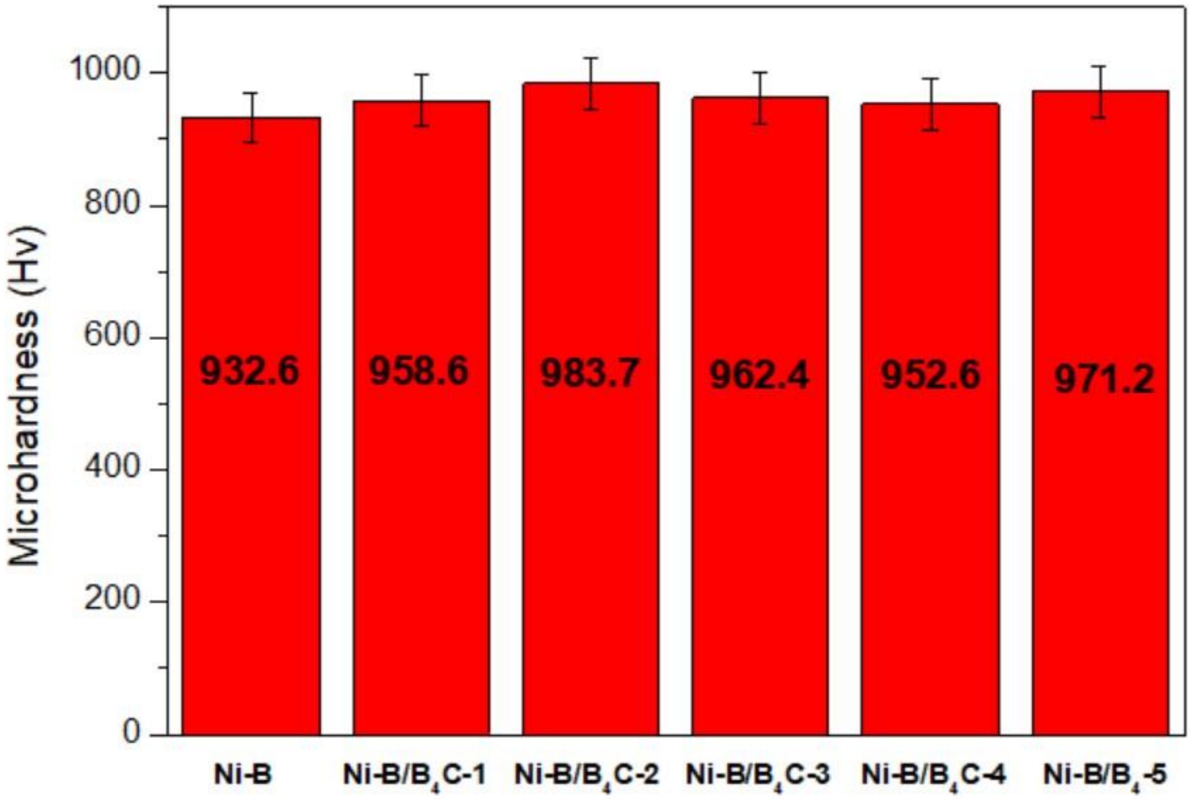

Figure 5. The micro-hardness of Ni-B alloy coatings and Ni–B/B_4C composite coatings electrodeposited from different added B_4C particles concentrations, the samples including: Ni-B, Ni-B/B_4C-1, Ni-B/B_4C-2, Ni-B/B_4C-3, Ni-B/B_4C-4 and Ni-B/B_4C-5.

Fig. 6 presents SEM morphologies of the worn surfaces of Ni-B alloy coatings and Ni-B/B_4C composite coating prepared by adding different concentrations of B_4C particles. Fig. 6(a) presents the worn surfaces of Ni-B alloy coatings, a typical adhesive wear occurred at Ni-B alloy coatings and caused it has the largest wear rate (5.6×10^{-4} mg/N·m). After the composite coatings prepared under the conditions of B_4C particle addition of 1 g/L, 2 g/L and 3 g/L (sample code: Ni-B/B_4C-1, Ni-B/B_4C-2, Ni-B/B_4C-3), it was found that the nodular structure formed on the surface of the composite coating due to the aggregation of B_4C particles can resist the wear of ceramic grinding balls and the composite coatings without peeling (Fig. 6(b), (c), (d)). When the B_4C particle addition concentration increase to 4 g/L and 5 g/L (sample code: Ni-B/B_4C-4, Ni-B/B_4C-5), the Ni-B/B_4C composite coatings occurred seriously peeling off which caused by the effect of adhesive wear (Fig. 6(e), (f)).

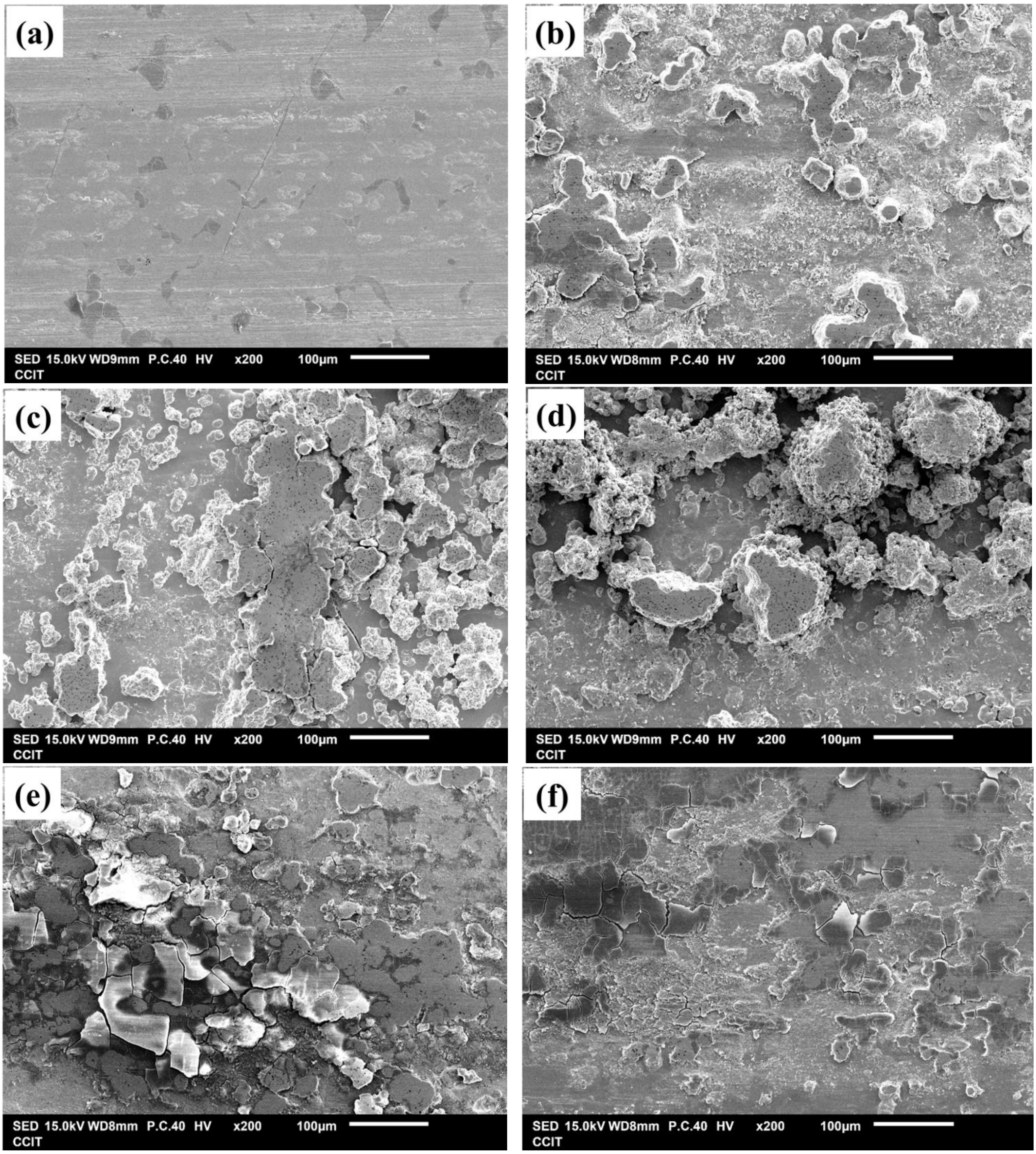

Figure 6. SEM morphologies of the worn surfaces of Ni-B alloy coatings and Ni–B/B_4C composite coatings electrodeposited from different added B_4C particles concentrations: (a) Ni-B, (b) Ni-B/B_4C-1, (c) Ni-B/B_4C-2, (d) Ni-B/B_4C-3, (e) Ni-B/B_4C-4 and (f) Ni-B/B_4C-5.

Table 2. Micro-hardness and wear resistance properties of Ni-B alloy coatings and Ni–B/B_4C composite coatings prepared with different concentrations of B_4C particles

Sample code	Micro-hardness (Hv)	B_4C content in the coatings (Vol.%)	Friction coefficient	Wear rate (mg/N·m)
Ni–B	932.6	0	0.545	5.6 E–4
Ni–B/B_4C-1	958.2	7.34	0.353	4.1 E–4
Ni–B/B_4C-2	983.7	15.2	0.358	2.7 E–4
Ni–B/B_4C-3	962.4	10.7	0.354	3.6 E–4
Ni–B/B_4C-4	963.6	10.3	0.341	4.5 E–4
Ni–B/B_4C-5	971.2	9.21	0.464	4.8 E–4

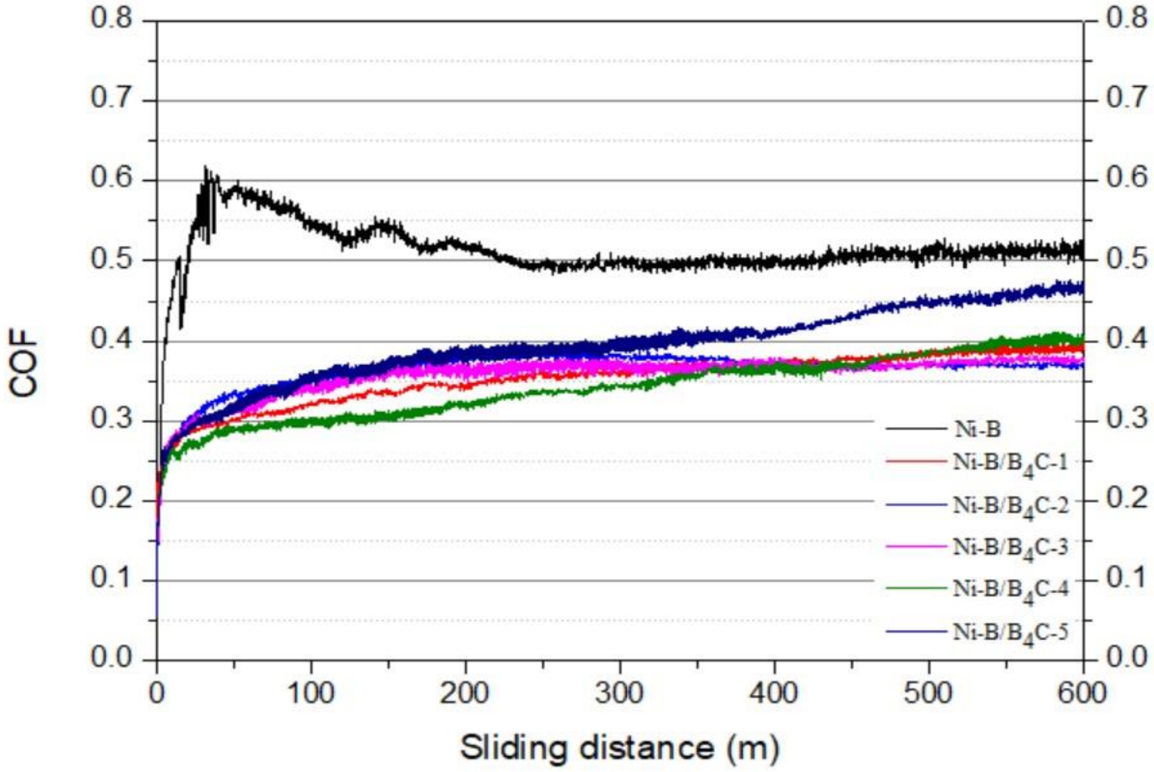

Figure 7. The friction coefficient curves of Ni-B alloy coatings and Ni–B/B_4C composite coatings electrodeposited from different added B_4C particles concentrations after sliding for 600 m, the samples including: Ni-B, Ni-B/B_4C-1, Ni-B/B_4C-2, Ni-B/B_4C-3, Ni-B/B_4C-4 and Ni-B/B_4C-5.

The wear rates of Ni-B/B_4C-1, Ni-B/B_4C-2, Ni-B/B_4C-3 were 4.1×10^{-4}, 2.7×10^{-4}, and 3.9×10^{-4} mg/N·m, respectively (as shown in Table 2). After the composite coatings prepared under the conditions of 4 g/L and 5 g/L (Ni-B/B_4C-4 and Ni-B/B_4C-5) were subjected to the wear test, it was found that the coating would peel off during the wear process, which increased the wear rate of the composite coating, and their wear rates were 4.5×10^{-4} and 4.8×10^{-4} mg/N•m. Moreover, the Ni-B alloy coatings has the biggest wear rate approximately at 5.6×10^{-4} mg/N·m. The reason for the above phenomenon can be attributed to the fact that the composite coatings prepared under the conditions of 2 g/L and 3 g/L have a relatively high content of B_4C particles (contents are 15.2 and 10.7 Vol.%). The contact area of the ceramic grinding ball is reduced, and the hard grinding debris will form a third body between the grinding ball and the surface of the coating, resulting in the effect of three-body wear, so that the friction coefficient is maintained at a low and stable state, and it also reduces the chance of the entire coating peeling off (Fig. 6). After the composite coatings prepared under the conditions of 4 g/L and 5 g/L were subjected to the wear test, it was found from the wear track photos that the coating produced adhesive wear during the wear process, resulting in the coating friction coefficient began to increase after a certain distance of wear (Fig. 7).

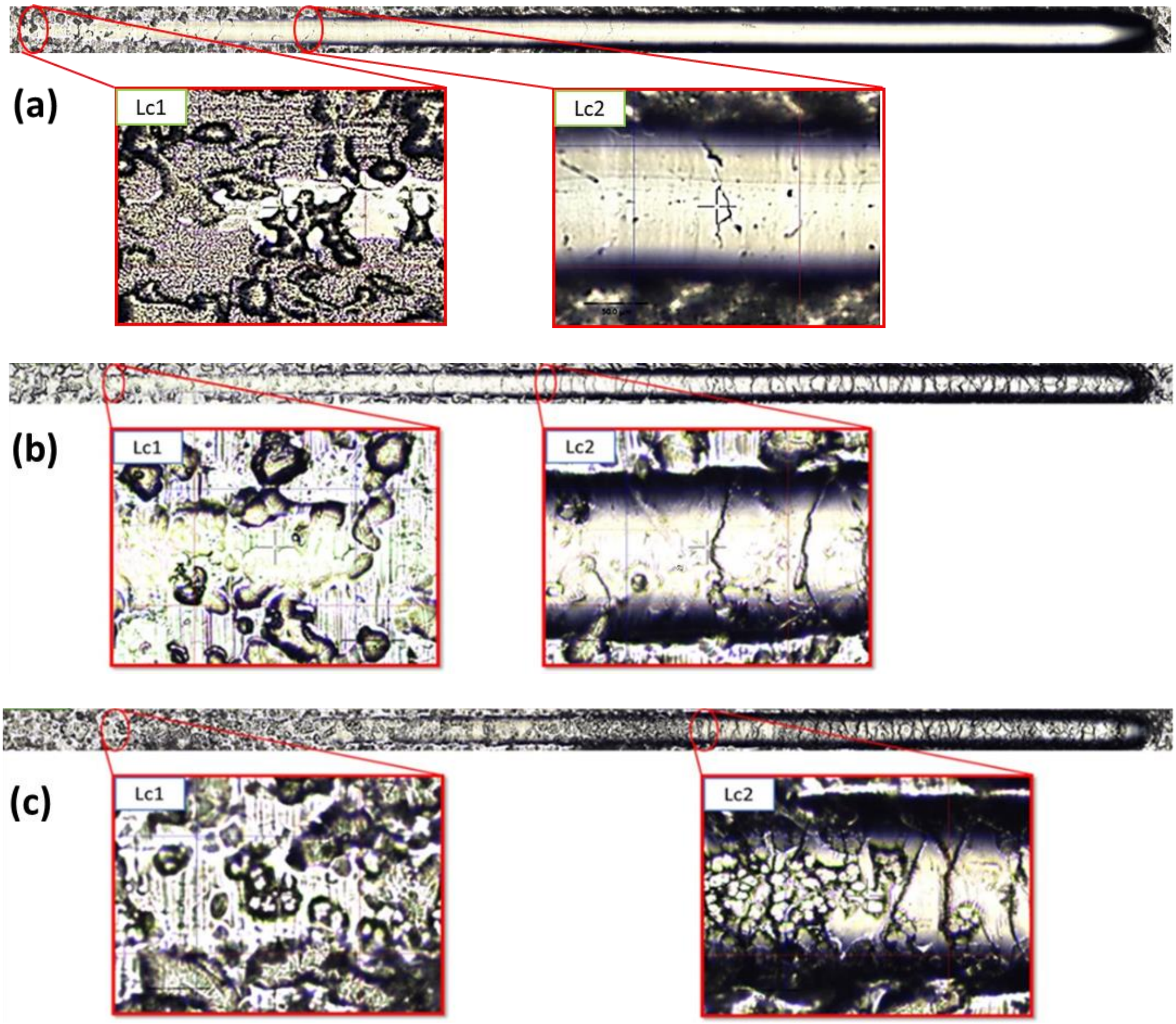

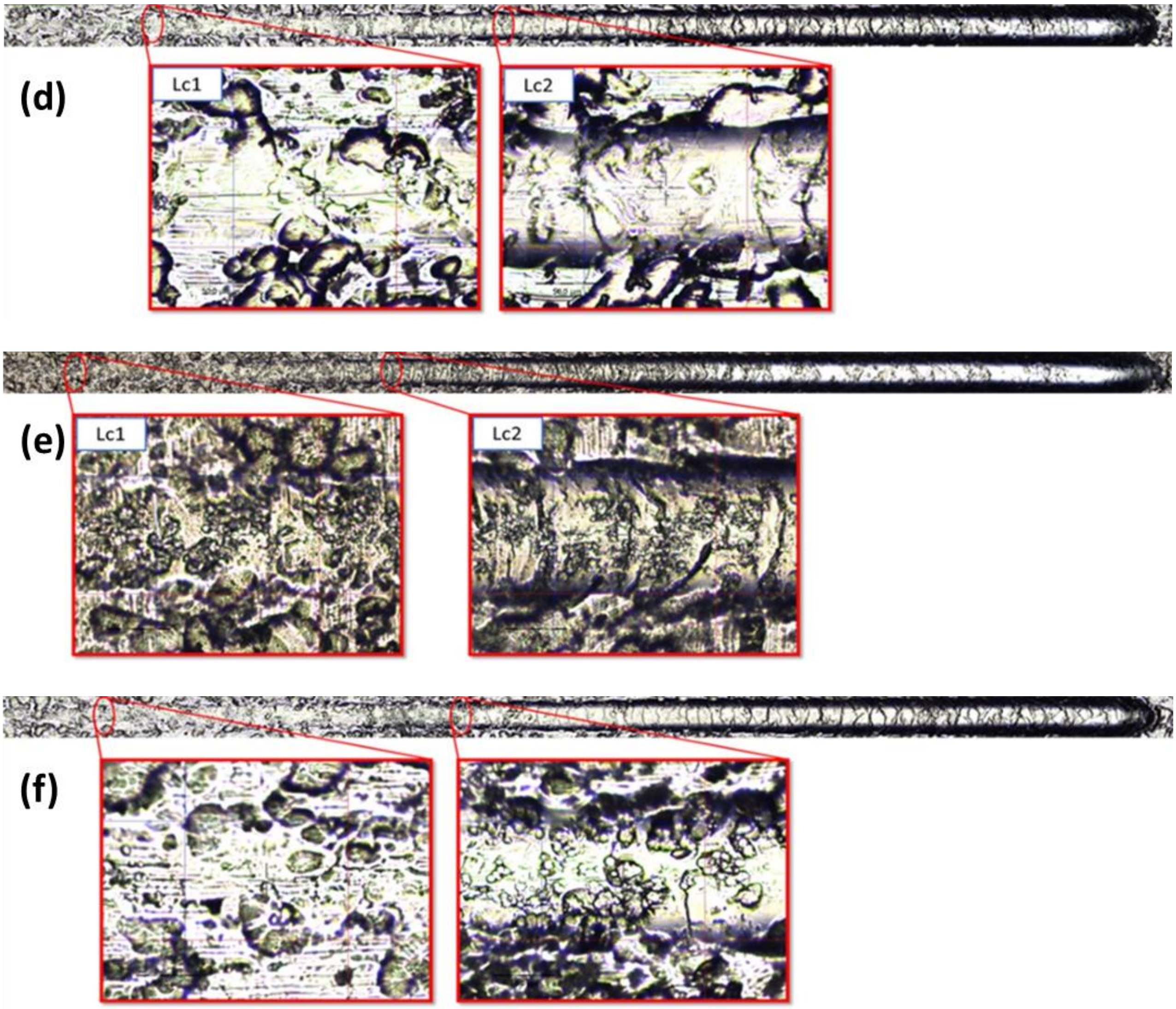

Figure 8. The scratch test images of Ni-B alloy coatings and Ni-B/B$_4$C composite coatings electrodeposited from different added B$_4$C particles concentrations: (a) Ni-B, (b) Ni-B/B$_4$C-1, (c) Ni-B/B$_4$C-2, (d) Ni-B/B$_4$C-3, (e) Ni-B/B$_4$C-4 and (f) Ni-B/B$_4$C-5.

Table 3. The analysis of critical load of Ni-B alloy coatings and Ni-B/B$_4$C composite coatings prepared with different concentrations of B$_4$C particles

Sample code	**L_{c1}**	**L_{c2}**	**Critical load (load of L_{c2})**
Ni–B	0.32 mm	1.56 mm	9.76 N
Ni–B/B$_4$C-1	0.52 mm	2.26 mm	14.08 N
Ni–B/B$_4$C-2	0.58 mm	3.48 mm	20.24 N
Ni–B/B$_4$C-3	0.71 mm	2.31 mm	14.39 N

Ni–B/B_4C-4	0.38 mm	1.71 mm	10.89 N
Ni–B/B_4C-5	0.70 mm	2.28 mm	14.2 N

Fig. 8 is a photo of the scratch test of the Ni-B alloy coatings and Ni-B/B_4C composite coating prepared by adding different concentrations of B_4C particles. The relevant scratch test properties are shown in Table 3. The Ni-B alloy coatings has the smallest critical load (9.76 N). The composite coating prepared with B_4C particle concentration of 2 g/L has the maximum Lc_2 value of 3.48 mm, and its critical load is 20.24 N. This indicates that the composite coating prepared under this condition has the best adhesion strength.

4. CONCLUSIONS

The effects of added concentration of B_4C particles on the corrosion resistance and wear resistance of Ni-B/B_4C composite coatings were investigated. The highest co-deposited amount of B_4C particles of Ni-B/B_4C composite coatings was 15.2 Vol.% when the addition concentration of B_4C particle is 2 g/L. The best corrosion resistance (i_{corr}=8.78×10^{-7} A/cm^2), wear rate (2.7×10^{-4} mg/N·m) and hardness (983.7 Hv) of the composite coatings are all occurred at the addition concentration of B_4C particle is 2 g/L. This can be attributed to the highest concentration of B_4C particles can reduce the formation of micro-cracks and enhance the corrosion resistance of coatings, the high amount of B_4C particles content can improve the wear resistance of coatings.

ACKNOWLEDGEMENTS
The authors thank the Ministry of Science and Technology of the Republic of China, Taiwan, for financially supporting this research under Contract nos. MOST- 110-2221-E-606 -002 and MOST- 111-2221-E-262 -007.

References

1. F. Zhang, Z. Yao, O. Moliar, X. Tao, C. Yang, *J. Alloys Compd.*, 830 (2020) 153785.
2. A.G. González-Gutiérrez, M.A. Pech-Canul, G. Chan-Rosado, P.J. Sebastian, *Fuel*, 235 (2019) 1361.
3. B. Yue, G. Zhu, Y. Wang, J. Song, Z. Chang, N. Guo, M. Xu, *J. Electroanal. Chem.*, 910 (2022) 116146.
4. H.H. Sheu, S.Y. Jian, M.H. Lin, C.I. Hsu, K.H. Hou, M.D. Ger, Int. J. Electrochem. Sci., 12 (2017) 5464.
5. N. Kothanam, K. Harachai, J. Qin, Y. Boonyongmaneerat, N. Triroj, P. Jaroenapibal, *J. Mater. Res. Technol.*, 19 (2022) 1884-1896.
6. Y. Wang, L. Guan, Z. He, S. Zhang, H. Singh, M. D. Hayat, C. Yao, *Mater. Des.*, 197 (2021)

109233.
7. K.H. Hou, H.T. Wang, H.H. Sheu, M.D. Ger, *Appl. Surf. Sci.*, 308 (2014) 372.
8. L. Bathini, M. J. N. V. Prasad, N. P. Wasekar, *Surf. Coat. Technol.*, in press (2022) 128728.
9. T. Man, C. D. Hu, H. C. Lu, Y.W. Chen, Y. Lin, H. Dong, *Mater. Today Commun.*, 31 (2022) 103244.
10. M. Romero-Romero, C. Domínguez-Ríos, R. Torres-Sánchez, A. Aguilar-Elguezabal, *Surf. Coat. Technol.*, 315 (2017) 181.
11. K. Krishnaveni, T.S.N. Sankara Narayanan, S.K. Seshadri, *Mater. Chem. Phys.*, 99 (2006) 300.
12. R.K. Saha, T.I. Khan, *Mater. Charact.*, 60 (2009) 1001.
13. E. Ünal, I.H. Karahan, *Surf. Coat. Technol.*, 333 (2018) 125.
14. I. Matsui, N. Omura, T. Yamamoto, Y. Takigawa, *Surf. Coat. Technol.*, 337 (2018) 411.
15. K.H. Lee, D. Chang, S.C. Kwon, *Electrochim. Acta*, 50 (2005) 4538.
16. H.H. Sheu, Y.C. Tzeng, J.H. Syu, *Mater. Lett.*, 238 (2019) 275.
17. Y.N. Bekish, S.K. Poznyak, L.S. Tsybulskay, T.V. Gaevskay, *Electrochim. Acta*, 55 (2010) 2223.
18. E. Beltowska–Lehman, A. Bigos, P. Indyka, M. Kot, *Surf. Coat. Technol.*, 211 (2012) 67.
19. N. Guglielmi, *J. Electrochem. Soc.*, 119 (1972) 1009.
20. J. P. Celis, J. R. Roos, C. Buelens, *J. Electrochem. Soc.*, 134 (1987) 1402.
21. B. J. Hwang, C. S. Hwang, *J. Electrochem. Soc.*, 140 (1993) 979.
22. P.C. Huang, K.H. Hou, J.J. Hong, M.H. Lin, G.L. Wang, *Wear*, 477 (2021) 203772.
23. H.H. Sheu, M.H. Lin, S.Y. Jian, T.Y. Hong, K.H. Hou, M.D. Ger, *Surf. Coat. Technol.*, 350 (2018) 1036.
24. L. Huang, Q. Dai, W. Huang, X. Wang, *Appl. Surf. Sci.*, 572 (2022) 151534.
25. H.T. Wang, H.H. Sheu, M.D. Ger, K.H. Hou, *Surf. Coat. Technol.*, 259 (2014) 268.
26. H.H. Sheu, Q.Y. Wang, P.C. Huang, A.Y. Cheng, Y.M. Liu, K.H. Hou, M.D. Ger, *Int. J. Electrochem. Sci.*, 16 (2021) 21049.
27. A.Y. Cheng, H.H. Sheu, Y.M. Liu, K.H. Hou, P.Y. Hsieh, M.D. Ger, *Int. J. Electrochem. Sci.*, 15 (2020) 68.
28. H.H. Sheu, T.T. Lin, M.D. Ger, *Int. J. Electrochem. Sci.*, 17 (2022) 22076.
29. C. A. Huang, C. K. Lin, C. Y. Chen, *Surf. Coat. Technol.*, 203 (2009) 3686.
30. S. Surviliene, L. Orlovskaja, G. Bikulcius, S. Biallozor, *Surf. Coat. Technol.*, 137 (2001) 230.
31. S. Surviliene, A. Lisowska-Oleksiak, V. Jasulaitiene, A.C. Esuniene, *Trans. IMF*, 83 (2005) 130.
32. S. Surviliene, V. Jasulaitiene, A. Lisowska-Oleksiak, V.A. Safonov, *J. Appl. Electrochem.*, 35 (2005) 9.
33. H.H. Sheu, C.E. Lu, K.H. Hou, M.L. Kuo, M.D. Ger, *J. Taiwan Inst. Chem. Eng.*, 48 (2015) 73.
34. A. Joseph, M. Narayanasamy, B. Kirubasankar, S. Angaiah, *ES Mater. Manuf.*, 2 (2018) 2.
35. Y. Zhang, L. Feng, W. Qiu, *J. Mater. Sci.*, 54 (2019) 9507.
36. V. N. Tseluikin, *Prot. Met. Phys. Chem. Surf.*, 52 (2016) 254.